H$_2$S Sensing Properties and Mechanism of Macroporous Semiconductor Sensors

T. Hyodo[a], S. Nonaka[a], Y. Shimizu[b], and M. Egashira[b]

[a] Graduate School of Science and Technology, Nagasaki University,
[b] Faculty of Engineering, Nagasaki University,
1-14 Bunkyo-machi, Nagasaki 852-8521, Japan

Macroporous (mp-) In$_2$O$_3$-based films with and without 1 wt% CuO loading were fabricated by a modified sol-gel technique employing polymethylmethacrylate microspheres as a template and their sensor responses to H$_2$S and the reaction behavior of H$_2$S over the sensor materials were investigated. Introduction of macropores into an In$_2$O$_3$ film and simultaneous loading of CuO on the In$_2$O$_3$ surface were enormously effective in improving the H$_2$S response. The large surface area of mp-In$_2$O$_3$ loaded with CuO, which increased the reactivity of CuO with H$_2$S, is probably the most important factor to enhance the H$_2$S response.

Introduction

Structural control of macropores as well as mesopores in gas-sensing materials is very essential for improving gas sensitivity and selectivity, because it provides suitable gas reactivity and diffusivity to semiconductor gas sensors. Therefore, we have so far developed mesoporous SnO$_2$ (> 300 m^2 g^{-1} even after calcination at 600ºC) (1) and its related materials (2-4) with high thermal stability and high specific surface area, and then demonstrated their potentials as gas sensor materials. In addition, we have recently fabricated various types of macroporous (mp-) oxide films, which have three-dimensionally (3D) ordered arrays of submicron-sized spherical pores, as promising gas-sensing materials by a modified sol-gel method (5-12) or some kinds of physical vapor deposition techniques (13, 14) employing polymetheylmethacrylate (PMMA) microsphere templates. In these studies, it was confirmed that introduction of well-developed macropores into host sensor materials was also greatly effective in improving their gas sensing performances. The present study has been focused on the evaluation of H$_2$S sensing properties of mp-oxide sensors and discussion of their sensing mechanism.

Experimental

An aqueous suspension containing non-cross-linked PMMA microspheres (Soken Chem. & Eng., Co. Ltd., 400 or 800 nm in diameter (d)) was dip-coated on an alumina substrate, on which interdigitated Pt electrodes had been printed, and then it was dried at room temperature to obtain a 3D self-assembly of PMMA microspheres. Then, a 0.5 mol dm^{-3} In(NO$_3$)$_3$ precursor solution was impregnated into the openings of the 3D self-assembly. In some cases, an appropriate amount of CuCl$_2$ was added to the precursor solution to fabricate the oxide film mixed with 1 mol% CuO. The PMMA-precursor composite films were heated at 600°C for 2 h to form macroporous structure reflecting the 3D self-assembly of PMMA microspheres. These macroporous film sensors obtained were denoted as mp(d)-In$_2$O$_3$ or mp(d)-CuO/In$_2$O$_3$. Typical thick film sensors without macropores (R-In$_2$O$_3$ or R-CuO/In$_2$O$_3$) were also fabricated for reference. These oxide

powders were prepared by hydrolysis of the above-mentioned precursor solutions, followed by firing at 600°C for 2 h. Then, the powder was mixed with an appropriate amount of organic lacquer, and the mixture was screen-printed on the above-mentioned substrate. These sensors were subjected to firing at 550°C for 5 h.

Sensing properties to 10 ppm H_2S of these sensors were measured in air in a temperature range of 200~500°C. The magnitude of H_2S response was defined as the ratio of sensor resistance in air (R_a) to that in 10 ppm H_2S balanced with air (R_g).

Catalytic combustion behaviour of 500 ppm H_2S over mp(d)-CuO/In_2O_3 and R-CuO/In_2O_3 were investigated to clarify the H_2S-sensing mechanism. However, the catalytic properties of macroporous films themselves were hard to be measured due to their small volume. Therefore, a macroporous disc (ca. 1 mm thick and 10 mm in diameter) was prepared, as described below. At first, a disc of PMMA microspheres was prepared by uniaxial pressing (ca. 1 kgf cm^{-2}). A small amount of the precursor solution stated above was permeated into the 3-D array of the PMMA disc in vacuo. They were calcined at 600°C for 2 h. On the other hand, powder of R-CuO/In_2O_3 was pressed into discs. The granules of about 0.5 g, which were prepared by pulverizing the discs obtained, were fixed in a glass reactor. Then, catalytic combustion behaviour of 390 ppm H_2S balanced with air over their granules was measured in a temperature range of 50~500°C at a flow rate of 50 cm^3 min^{-1} by using a gas chromatography-mass spectrometer (GC-MS, Shimadzu, QP-5050A). Temperature programmed desorption (TPD) spectra of SO_2 from mp(d)-CuO/In_2O_3 and R-CuO/In_2O_3 pretreated with 390 ppm H_2S balanced with air at 200°C for 3 h was carried out at a heating rate of 5°C under a He stream at a flow rate of 50 cm^3 min^{-1} by employing the same experimental setup as described above.

Specific surface area and pore size distribution of the granules of mp(d)-CuO/In_2O_3 and R-CuO/In_2O_3 were measured by a BET method using a N_2 sorption isotherm (Micromeritics, TriStar 3000). Morphology of macroporous films was observed by a scanning electron microscope (SEM, Hitachi, S-2250N) and a transmission electron microscope (TEM, JEOL, JEM2010-HT). Chemical binding states of constituent elements of R-CuO/In_2O_3, which was pretreated with and without 390 ppm H_2S balanced with air at 200°C for 0.5 and 10 h as well as treated under the same conditions as those for the TPD measurement, were characterized by X-ray photoelectron spectroscopy using MgK_α radiation (XPS, Shimadzu, ESCA-850), in which the binding energy was calibrated using the C1s level from usual contamination (284.5 eV).
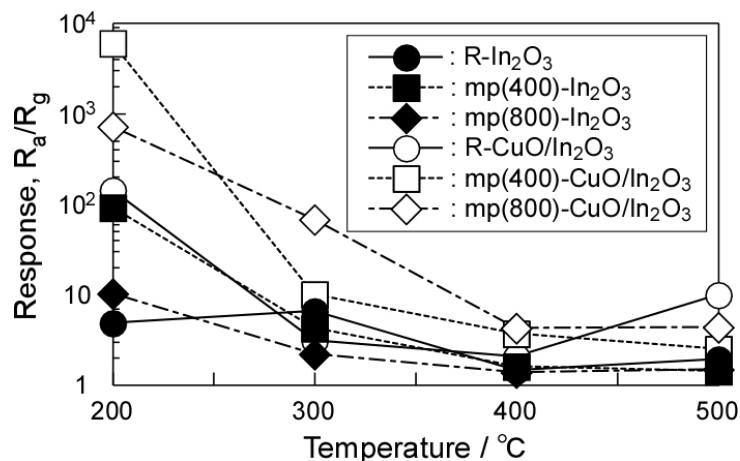
Figure 1. Temperature dependence of responses to 10 ppm H_2S of several sensors.

Results and Discussions

Temperature dependence of H₂S responses of the representative sensors fabricated is shown in Fig. 1. Addition of CuO to In₂O₃ improved the H₂S response of all sensors, as reported by Tamaki et al. (15, 16). Besides, introduction of macropores was largely effective in enhancing the response, especially for mp(d)-CuO/In₂O₃ sensors at temperatures of 300°C or less.

(a) mp(400)-CuO/In₂O₃ (b) mp(800)-CuO/In₂O₃ (c) R-CuO/In₂O₃
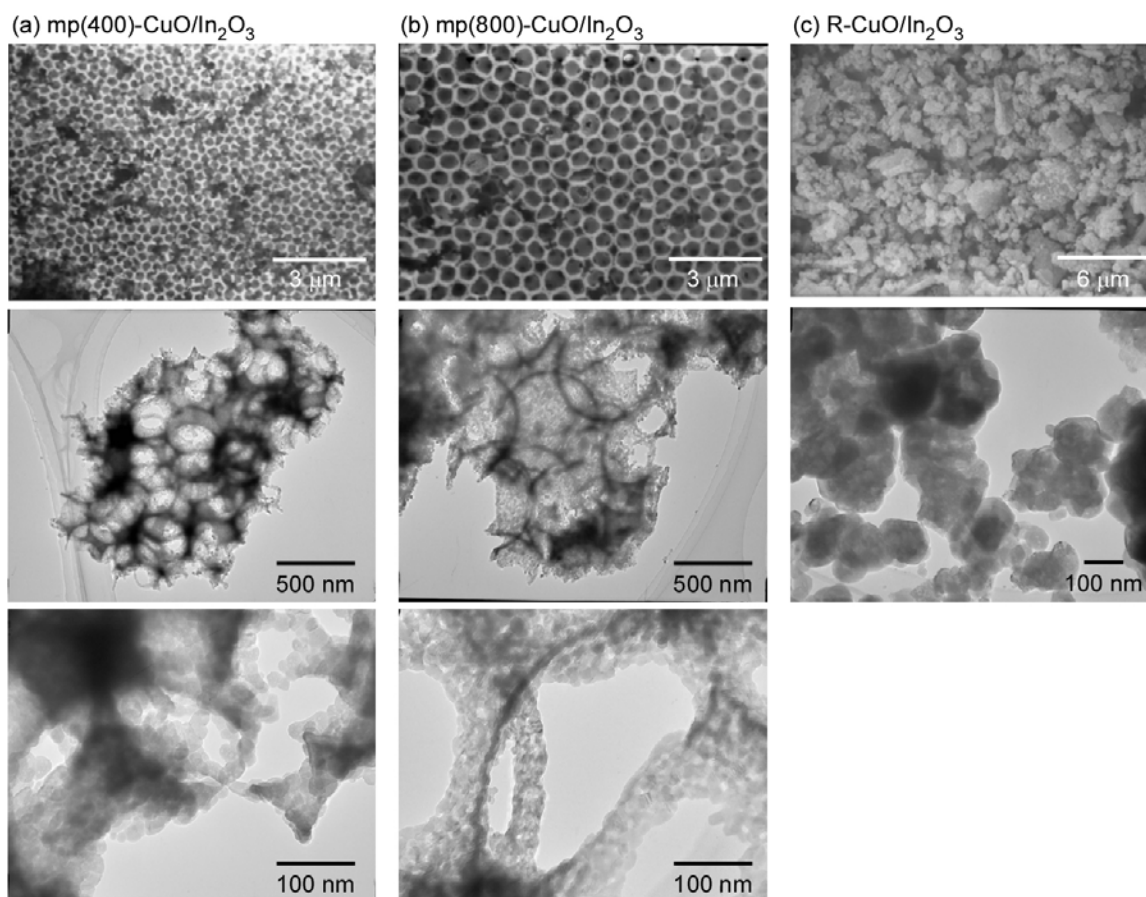
Figure 2. SEM and TEM photographs of mp(d)-CuO/In₂O₃ (d = 400 and 800 nm) and R-CuO/In₂O₃.

SEM and TEM photographs of CuO/In₂O₃ films with and without macropores are shown in Fig. 2. Well-developed and spherical macropores were observed on the surfaces of mp(400)-CuO/In₂O₃ and mp(800)-CuO/In₂O₃, and the spherical macropores reflecting the shape of the PMMA microspheres used were interconnected each other with small pores. The inner diameter of spherical macropores was ca. 300 and 600 nm with some exceptions for mp(400)-CuO/In₂O₃ and mp(800)-CuO/In₂O₃, respectively, and the size of both macropores reduced to ca. 80% of the size of each PMMA microsphere template. TEM photographs showed that the bulk of these macroporous films was also constituted with typically spherical macropores and the oxide walls around the macropores were constructed with nanoparticles of 17~20 and 12~15 nm in diameter for mp(400)-CuO/In₂O₃ and mp(800)-CuO/In₂O₃, respectively. In addition, the formation of well-developed mesopores was confirmed among these nanoparticles of both macroporous films. On the other hand, the surface of R-CuO/In₂O₃, which was

constituted with micron-size agglomerates, was enormously rough, and the TEM photograph showed that the particles were much larger than those of the macorporous films.
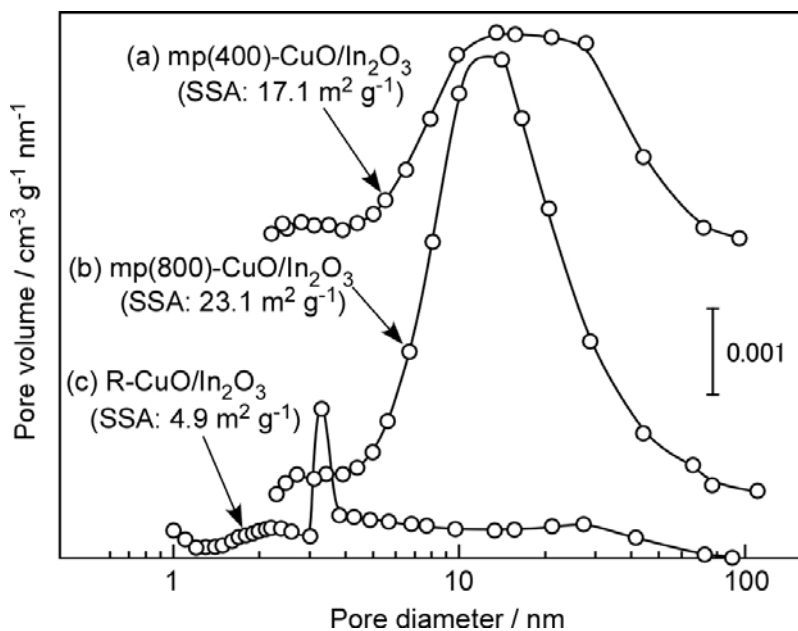
Figure 3. Pore size distributions of mp(d)-CuO/In$_2$O$_3$ (d = 400 and 800 nm) and R-CuO/In$_2$O$_3$.
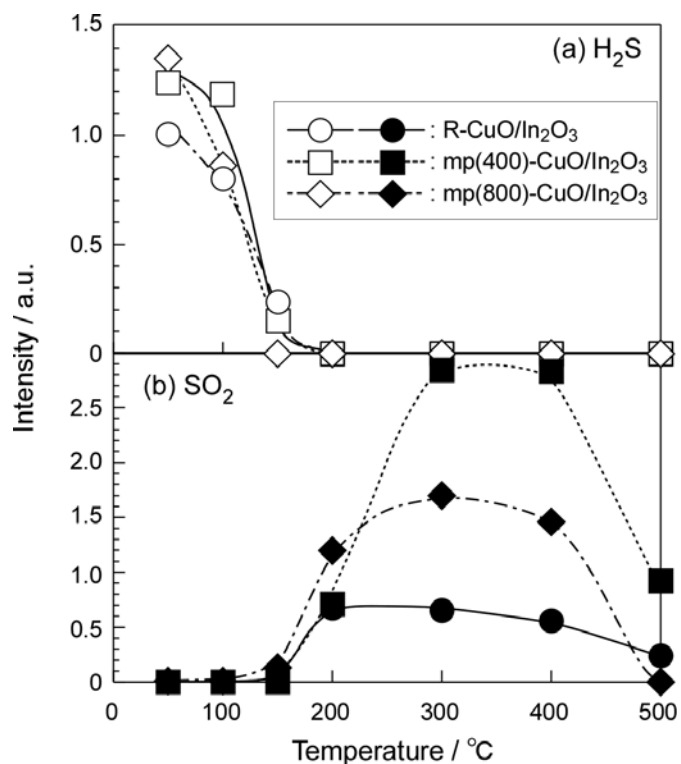
Figure 4. Catalytic combustion behavior of 390 ppm H$_2$S in air over mp(d)-CuO/In$_2$O$_3$ (d = 400 and 800 nm) and R-CuO/In$_2$O$_3$.

Figure 3 shows pore size distribution obtained from N_2 desorption behavior and specific surface area (SSA) of the three kinds of CuO/In_2O_3. mp(800)-CuO/In_2O_3 has a larger pore volume with a narrower pore size distribution centered at a pore diameter of ca. 12 nm and a larger surface area (23.1 m^2 g^{-1}) than those of mp(400)-CuO/In_2O_3 with broadly-distributed pores around 10~30 nm and a surface area of 17.1 m^2 g^{-1}. On the other hand, R-CuO/In_2O_3 had only a little and narrow peak at a diameter of ca. 3~4 nm, which seemed to be derived from bottleneck-type mesopores, with a small surface area (4.9 m^2 g^{-1}). By referring to such meso- and macro-structural characteristics shown in Figs. 2 and 3, small particle size, well-developed porous structure and large specific surface area of mp(d)-CuO/In_2O_3 are considered to be very effective for the improvement of H_2S-sensing properties.

Catalytic combustion behavior of 390 ppm H_2S in air over mp(d)-CuO/In_2O_3 and R-CuO/In_2O_3 powders was measured to clarify the above sensor behavior (see Fig. 4). It was confirmed that H_2S was oxidized and then SO_2 was produced in the temperature range higher than ca. 200°C. Figure 5 shows TPD spectra of SO_2 from the mp(d)-CuO/In_2O_3 and R-CuO/In_2O_3 powders pretreated with 390 ppm H_2S balanced with air at 200°C for 3 h. Desorption of SO_2 was observed in the temperature range higher than ca. 300°C. Figure 6 shows XPS spectra of Cu2$p_{3/2}$ and S2p of R-CuO/In_2O_3 as a representative sample before and after the H_2S treatment and after the TPD measurement. As for Cu2$p_{3/2}$, peak B at 933.8 eV which is originated from CuO (16) appeared before the H_2S treatment. The peak B decreased after the H_2S treatment for 0.5 h and more, and then peak A at 933.0 eV originated from CuS (16) became the main peak after the H_2S treatment for 10 h. As for S2p, peaks C and D assigned to S2$p_{3/2}$ and S2$p_{1/2}$ of CuS, respectively, were obvious after the H_2S treatment for both 0.5 and 10 h, with a small peak E originated from a sulfate or sulfite (S^{6+}) component. The peaks C and D increased with increasing the H_2S treatment time. No peaks originated from SO_2 (S^{4+}) species could be confirmed after the H_2S treatment. After the TPD measurement, on the other hand, the peak B became the main peak along with a decrease in peak A, the peaks C and D disappeared and the peak E increased significantly.
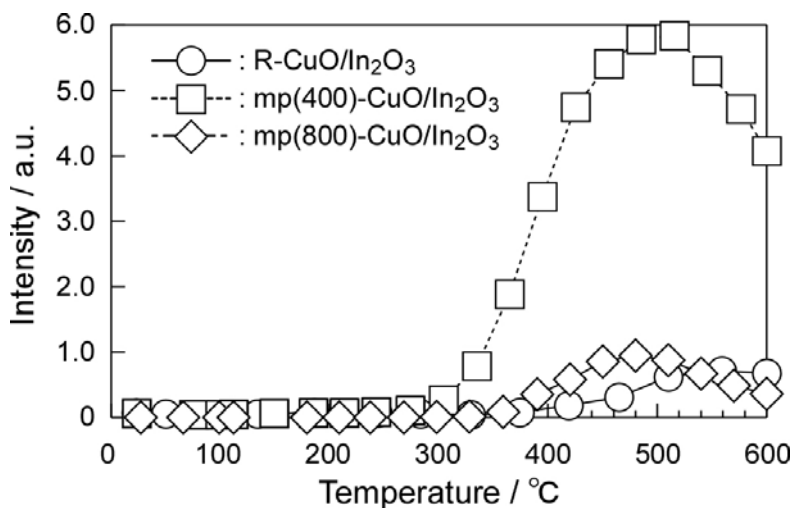
Figure 5. TPD spectra of SO_2 from mp(d)-CuO/In_2O_3 (d = 400 and 800 nm) and R-CuO/In_2O_3 pretreated with 390 ppm H_2S at 200°C for 3 h.

These results mean that CuS was easily produced by the reaction of H_2S molecules with CuO in H_2S balanced with air at 200°C, as also reported by Katti et al. (17) and Niranjan et al. (18). Simultaneously, the H_2S molecules are oxidized to SO_2 at the same atmosphere, but such S^{4+}-species are not adsorbed on the oxide surface (compare Fig. 4 with Fig. 6). On the other hand, the most part of SO_2 desorbed in the temperature range higher than ca. 300°C in TPD measurement (Fig. 5) is considered to be originated from those produced by the re-oxidation of CuS. Chemisorbed and/or lattice oxygen of In_2O_3 might react with CuS during the heating process. The large amount of SO_2 desorbed from mp(d)-CuO/In_2O_3 is ascribed reasonably to its relatively large surface area, in comparison with that of R-CuO/In_2O_3. The larger the surface area, the smaller the CuO particles dispersed on the surface of In_2O_3. This leads to an increase in effective volume of CuO to be reacted with H_2S and then larger H_2S response.
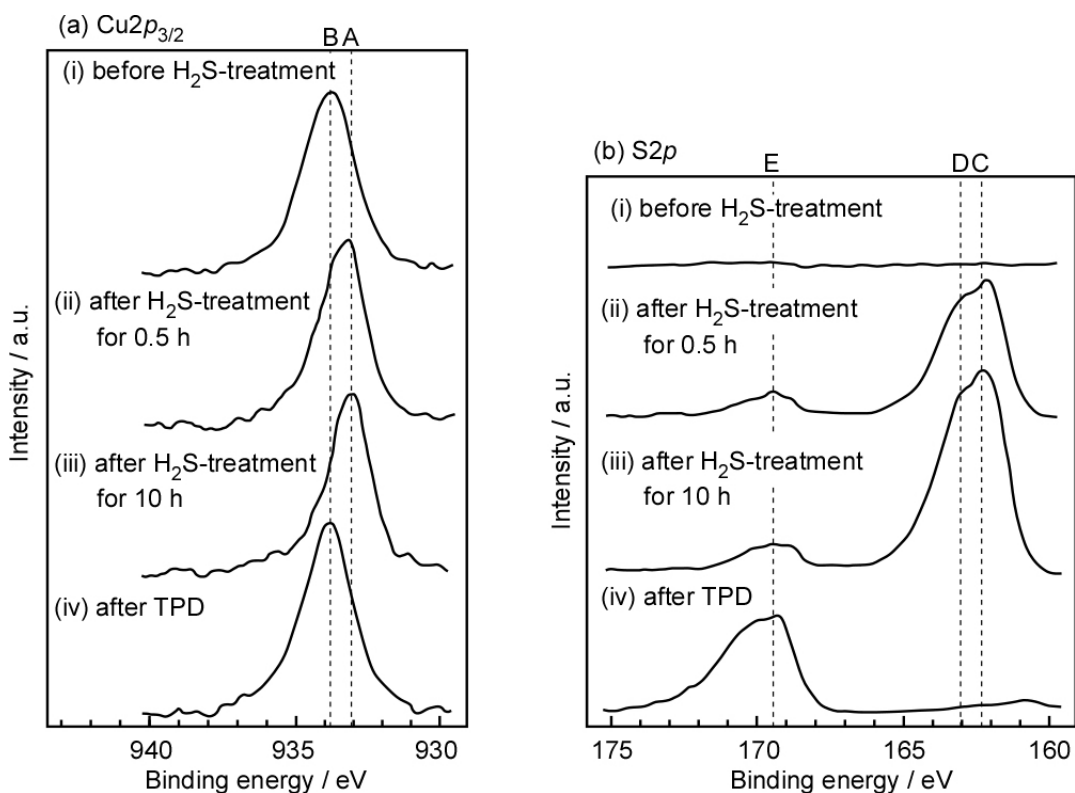
Figure 6. XPS spectra of (a) $Cu2p_{3/2}$ and (b) S2p of R-CuO/In_2O_3 before and after H_2S treatment, along with that after TPD measurement.

Conclusions

Macroporous In_2O_3-based films could be fabricated by a modified sol-gel technique employing two kinds of PMMA microsphere templates (d: 400 or 800 nm). Their films were constructed with spherical macropores interconnected each other with small pores and the oxide frameworks containing nanoparticles and mesopores. In addition, they showed a large surface area with well-developed mesopores among nanoparticles in the oxide frameworks. CuO loaded on the surface of In_2O_3 was confirmed to be converted to CuS by the reaction with H_2S molecules, from the experimental results of catalytic combustion, TPD and XPS measurements. The large surface area of mp(d)-CuO/In_2O_3 promoted the reaction of CuO with H_2S and then improved the H_2S response.

Acknowledgments

References

1. T. Hyodo, N. Nishida, Y. Shimizu, and M. Egashira, *Sens. Actuators B*, **83**, 209 (2002).
2. T. Hyodo, S. Abe, Y. Shimizu, and M. Egashira, *Sens. Actuators B*, **93**, 590 (2003).
3. Y. Shimizu, A. Jono, T. Hyodo, and M. Egashira, *Sens. Actuators B*, **108**, 56 (2005).
4. Y. Shimizu, K. Tsumura, T. Hyodo, and M. Egashira, *IEEJ Trans. SM*, **125**, 70 (2005).
5. K. Sasahara, T. Hyodo, Y. Shimizu, and M. Egashira, *J. Eur. Ceram. Soc.*, **24**, 1961 (2004).
6. T. Ishibashi, T. Hyodo, Y. Shimizu, and M. Egashira, in *Chemical Sensors VI/2004*, C. Bruckner-Lea, P. Vanýsek, G. Hunter, M. Egashira, N. Miura, and F. Mizutani, Editors, PV 2004-08, p. 28, The Electrochemical Society Proceedings Series, Honolulu, HI (2004).
7. T. Hyodo, K. Sasahara, Y. Shimizu, and M. Egashira, *Sens. Actuators B*, **106**, 580 (2005).
8. H. Seh, T. Hyodo, Y. Shimizu, and M. Egashira, *Sens. Actuators B*, **108**, 547 (2005).
9. Y. Takakura, T. Hyodo, Y. Shimizu, and M. Egashira, *IEEJ Trans. SM*, **128**, 137 (2008).
10. M. Morio, T. Hyodo, Y. Shimizu, and M. Egashira, in *Proc. Nagasaki Symp. Nano-Dynamics 2008*, p. 32, Nagasaki, Japan (2008).
11. S. Nonaka, T. Hyodo, Y. Shimizu, and M. Egashira, *IEEJ Trans. SM*, **128**, 141 (2008).
12. T. Hyodo, J. L. Hertz, and H. L. Tuller, in *Chemical Sensors VI/2004*, C. Bruckner-Lea, P. Vanýsek, G. Hunter, M. Egashira, N. Miura, and F. Mizutani, Editors, PV 2004-08, p. 10, The Electrochemical Society Proceedings Series, Honolulu, HI (2004).
13. I.-D. Kim, A. Rothchild, T. Hyodo, and H. L. Tuller, *Nano Letters*, **6**, 193 (2006).
14. J. Tamaki, T. Maekawa, N. Miura, and N. Yamazoe, *Sens. Actuators B*, **9**, 197 (1992).
15. T. Maekawa, J. Tamaki, N. Miura, and N. Yamazoe, *J. Mater. Chem.*, **7**, 1259 (1994).
16. S. K. Chawla, N. Sankarraman, and J. H. Payer, *J. Electron Spectrosc. Relat. Phenom.*, **61**, 1 (1992).
17. V. R. Katti, A. K. Debnath, K. P. Muthe, M. Kaur, A. K. Dua, S.C. Gadkari, S. K. Gupta, and V. C. Sahni, *Sens. Actuators B*, **96**, 245 (2003).
18. R. S. Niranjan, K. R. Patil, S. R. Sainkar, and I. S. Mulla, *Mater. Chem. Phys.*, **80**, 250 (2003).